A micromechanical switchable hot spot for SERS applications

Denys Naumenko,[1] Valeria Toffoli,[1] Silvio Greco,[1,2] Simone Dal Zilio,[1] Alpan Bek,[3] and Marco Lazzarino[1]
[1]*CNR-IOM laboratorio TASC, SS 14 km 163.5, 34149 Trieste, Italy*
[2]*Graduate School of Nanotechnology, University of Trieste, P.le Europa 1, 34143 Trieste, Italy*
[3]*Department of Physics, Middle East Technical University, 06800 Ankara, Turkey*

(Received 19 August 2016; accepted 21 September 2016; published online 29 September 2016)

Hot spots are defined as nanostructures of noble metal able to locally enhance the electromagnetic field of several orders of magnitude and to confine this effect to a region for several orders of magnitude smaller than the light wavelength. Hot spots are particularly important for the surface enhanced Raman spectroscopy applications, in which the field enhancement is used to amplify the usually weak Raman scattering signal. The hot spots are mostly generated between two or more plasmonic nanostructures separated by nanometric gaps. Several strategies are used to design and realize the hot spots, both in solution, using the noble metal nanoparticles, and on surfaces, using nanolithography and evaporation. In this paper, we demonstrated the fabrication of a nanomechanical plasmonic device for Raman spectroscopy, in which the hot spots are switched on when biased at the resonant frequency and switched off when the actuation signal is removed. *Published by AIP Publishing.* [http://dx.doi.org/10.1063/1.4964123]

Plasmonic resonances can be used to engineer the spatial distribution of the electromagnetic field (EMF) intensity at optical frequencies. In particular, the nanostructures of noble metal are able to locally enhance the EMF of several orders of magnitude and to confine this effect to a region for several orders of magnitude smaller than the light wavelength: these structures were named hot spots in a seminal paper by Stockman and coworkers.[1] Hot spots are extremely useful in all those non linear processes that require high EMF intensities such as Raman scattering. The use of hot spot rich substrates enabled the development of the surface enhanced Raman scattering technique (SERS) that demonstrated the single molecule sensitivity;[2] on the other hand, the use of a plasmonic probe in the tip enhanced Raman scattering (TERS) microscope enabled chemical mapping with spatial resolution of few nanometers.[3]

Single nanoparticles may provide SERS enhancements of the order of 10^3,[4] while designing nanoparticle distance with sub-nm gap enhancement of 10^9 was demonstrated.[5] In a hot spot, both the intensity and the wavelength of the resonance frequency depend on the size, shape and separation between the nanoparticles. The latter dependence in particular, has been used to create the so-called plasmonic rulers, nanostructures, in which a nanometric tuning of the interparticle distance is converted into a more directly measurable spectral shift.[6]

This property of the hot spot has recently been addressed in order to tune the plasmonic resonance of a substrate as function of the change of an external parameter. The reversible tuning of the plasmonic response was driven by the magnetic,[7] thermal,[8,9] pH[10] and biochemical interactions.[11]

In this paper, we use a micromechanical approach to reversible switch the effect of a plasmonic hot spot.

Micromechanical systems (MMS) are a broad family of devices characterized by microfabricated movable parts that may act as switchable, actuating or sensing elements in a transduction scheme. Cantilevers are the simplest examples of MMS: they are used as probes in the atomic force microscopes,[12] as static molecular sensors,[13] and as dynamic mass sensors.[14] In the latter applications, a cantilever is brought in oscillation at its resonance frequency by an external actuation signal and the precise value of the resonance frequency, which depends on the square root of the adsorbed mass, is measured. In order to be operated with the requested precision, cantilever interactions with the environment should be minimized, although gentle coupling with other cantilevers, of degenerate[15] or independent resonance frequency,[16] could be exploited in the particular cases.

When the cantilever interaction becomes extremely strong as for the presence of a physical boundary that limits mechanically the oscillation amplitude, an interesting case is developed, known as an impact oscillator (IO).[17] The main characteristics of the IO system are (i) a stiffening of the oscillator elastic constant proportional to the interaction with the steady boundary, (ii) a marked bistability, and (iii) a leveling of the oscillation amplitude because of the impact with the mechanical boundary. Although IO has been extensively investigated mathematically and with mm-sized mechanical models,[18] few attempts have been made to design and investigate its micromechanical counterpart.[19] In particular, the role played by the surface interactions, dominant at the micro and nanoscale, have not been investigated yet.

In order to design the micromechanical hot spots that could be exploited in a common optical configuration, the pillar geometry introduced by our group[20,21] is particularly interesting since pillars oscillate in the observation plane. In plane, hot spots are therefore created between two noble metal coated pillars that are separated at rest by a distance larger than the minimal plasmon coupling and that oscillate at an amplitude large enough to get in touch. We fabricated several arrays of pillars separated by a 100 nm gap from a steady wall, a typical IO configuration. A bright field optical top view of one array is given in Fig. 1(a); a tilted SEM detail of one pillar is given in Fig. 1(b). The fabrication

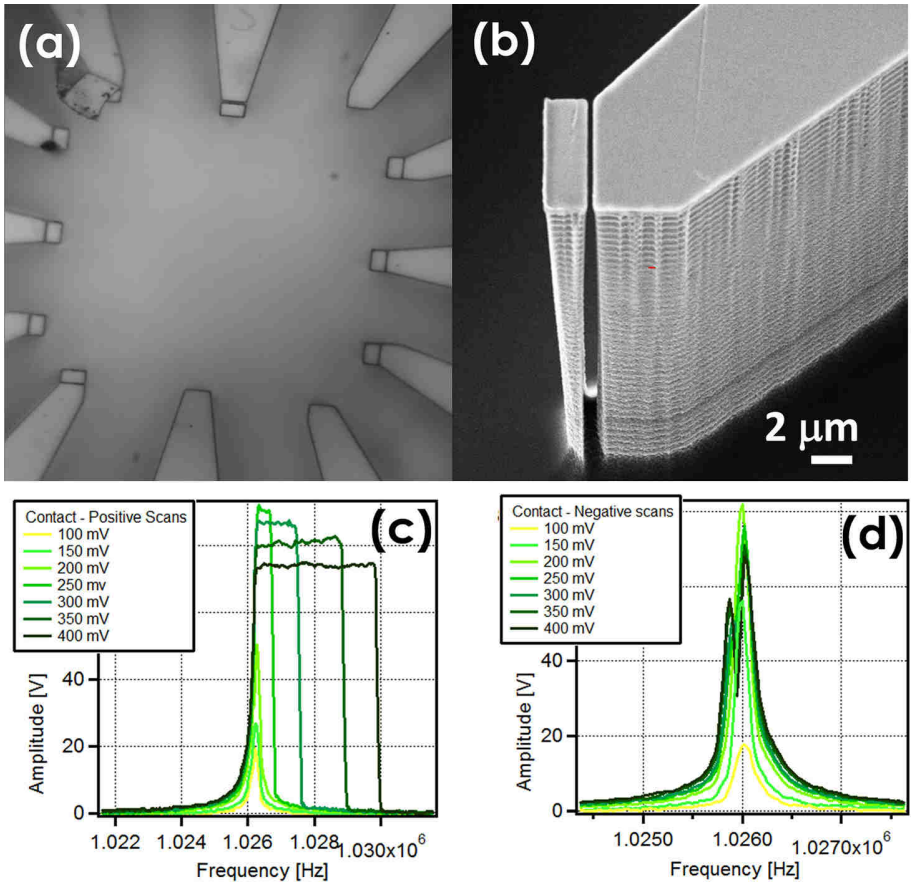

FIG. 1. (a) Bright field optical microscope image—top view—of an array of pillars used to generate micromechanical switchable SERS active plasmonic hot spots. (b) Scanning electron microscope image–side view–on one pillar from the array: the gap between the pillar top (left) and the steady wall is about 100 nm. (c) Pillar oscillation amplitude for increasing frequency in vacuum at increasing actuation voltage. For voltages exceeding 200 mV, the pillar impacts against the steady wall and a significant stiffening is observed. (d) Pillar oscillation amplitude for decreasing frequency in vacuum at decreasing actuation voltage: the stiffening does not affects the resonance peak shape.

details are described in Ref. 21. Briefly, starting from a ⟨100⟩, PMMA coated, p-doped silicon wafer, the selected pattern was written by e-beam lithography and transferred by development, 30 nm Cr deposition and subsequent lift off. The pillars were etched in an inductive coupled reactor using a C_4F_8:Ar and SF_6:Ar Bosch like reactive ion etching protocol, suitably modified to achieve a slight undercut and complete etching in the gap.

The pillars were mechanically characterized in vacuum (10^{-6} mbar) brought in oscillation around their first resonant mode with a piezo driven by an arbitrary function generator; the pillar oscillation amplitude was recorded with the optical lever approach, as described in more detail in Ref. 20. In Fig. 1(c), the pillar oscillation amplitude is plotted versus the oscillation frequency for increasing the actuation amplitudes. During the measurement, the frequency was scanned upward from lower to higher frequencies. In Fig. 1(d), the same amplitudes are plotted for downward scanned frequencies. Up to 200 mV of actuation amplitude, the pillar behaves like an isolated one,[20] with the resonance amplitude that follows a Lorentzian curve. For an actuation of 250 mV and above, a typical Duffing behavior is observed, with the resonance frequencies increasing with the actuation amplitude for upward frequency scans, indicating a resonator stiffening, while no effect is observed for the downward frequency scan.[22,23] However, on the contrary with isolated oscillator (as shown in supplementary material, Fig. S1), for the actuation of 250 mV and above, the oscillation amplitude does not increase. We interpret the data in terms of an ideal impact oscillator. At actuation of 250 mV, the pillar grazing impacts the steady wall. At larger actuation, the impact becomes more important and, as a consequence of the stiffening effect, the resonance frequency increases. However, due to the space constraint, the oscillation amplitude remains the same. Although the motion in an impact oscillator is chaotic, we can assume that, by increasing the actuation strength, the fraction of the oscillation period in which the pillar is in contact with the rigid wall increases, as indirectly suggested by the pillar stiffening increase.

A thin layer of Cr/Au (2 nm:40 nm) was deposited on the top surface of the device by thermal evaporation. The evaporation direction was tilted 45° off the normal direction and moved along 4 orthogonal directions on the azimuthal plane in order to deposit the metal layer on the pillar and wall sides. When the device is actuated, the edges of the film on the facing sides of the pillar and the steady wall are thus separated by a gap that varies from 0 nm to about 200 nm with the same frequency of the pillar resonance.

To investigate the effective formation of frequency modulated hot spots in the gap and their possible application for Raman spectroscopy, we evaporated a thin layer of pentacene and then we collected the local Raman spectra in correspondence with the hot spots. In this case, the evaporation direction was tilted 30° off the normal direction and moved along 4 orthogonal directions on the azimuthal plane; in each deposition, a 2.0 nm thick layer was deposited. We choose pentacene for two reasons: (a) Thin layers of pentacene have a strong absorption peak around 660 nm,[24,25] the laser wavelength used in these experiments (see also Fig. S2), which provides a higher resonant SERS (SERRS) signal; (b) pentacene can be

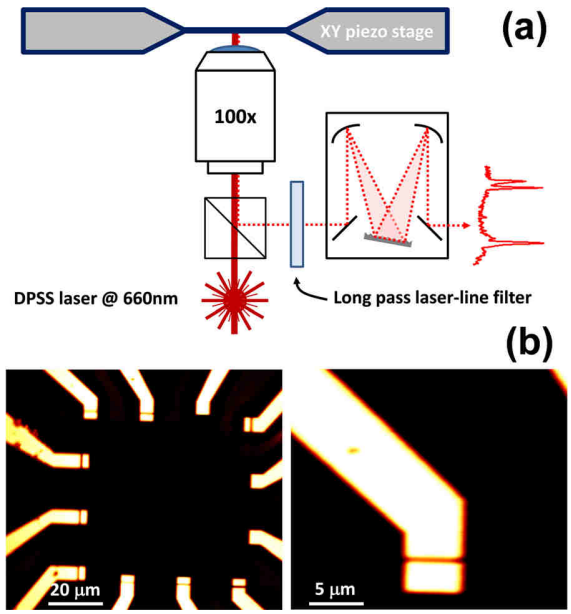

FIG. 2. (a) Schematic description of the sample scanning confocal microscope (SSCM) used in the experiment: a laser light is focused on the sample by a high magnification objective that is also used to collect the reflected light. A neutral beam splitter is used to direct the reflected light to the entrance of a monochromator. A razor-edge long pass filter is used to reject the Rayleigh reflection when the Raman spectra are acquired. (b) and (c) SSCM images of the pillar array of Fig. 1 recorded setting the spectrometer to the 0th diffraction order, removing the long pass filter and collecting the Rayleigh scattered light. Notice that here the 100 nm wide gap is clearly distinguishable.

deposited via thermal evaporation ensuring a morphology independent uniformity; other dyes, usually adopted as SERRS reporters such as Rhodamine or Nile Blue, are deposited from solution and, therefore, the surface tension effects on structured surfaces could lead to a local accumulation that may result in systematic errors in the evaluation of the SERRS intensity. In order to localize the Raman signal, a sample scanning confocal microscopy (SSCM) approach was used. The set-up is sketched in Fig. 2(a). A 1 MHz bandwidth 660 nm diode-pumped solid-state laser is focused on the sample with a 100×, 0.8 NA air objective. The reflected light is directed by a single-edge dichroic beamsplitter into the entrance of a 750 mm long monochromator equipped with a TE cooled EM-CCD camera. The sample is mounted on to a 100 μm × 100 μm piezo scanner. When collecting the reflected light images, the monochromator was set on the Rayleigh wavelength at 660 nm. To collect the Raman spectra, a long-pass edge filter was used to reject the Rayleigh light and the monochromator wavelength was adjusted accordingly. A representative SSCM Rayleigh image is displayed in Fig. 2(b).

The Raman spectra of pentacene were recorded at four different locations along the gap with and without actuation, maintaining the laser polarization perpendicular to the gap, so that the hot spot formation was maximized. Since here the device is operated in the presence of air damping, the voltage required is a factor 20 higher. The spectra are displayed in Fig. 3(a), while the acquisition locations are displayed in Fig. 3(b): in one of the edges, a two-fold Raman intensity increase was observed. While keeping the laser focused on that edge, the Raman spectra at increasing actuation voltage were recorded. Spectra are displayed in Fig. 4(a). Fig. 4(b) displays the area of the main three Raman peaks of pentacene as a function of the actuation voltage. The areas experience comparable enhancement as a function of the actuation voltage, as expected for SERRS condition, in which the main effect is electromagnetic and not chemical. Indeed, the mechanical actuation induces the enhancement of the local EM field via the formation of hot spots, but it does not change the chemistry between the pentacene and the Au substrate.

The Raman spectra were acquired also on the pillar top surface far from the gap and with polarization parallel to the gap, both with and without the maximum actuation. Expectedly, in neither of the cases, significant differences were recorded. Data are shown in supplementary material, Fig. S3.

Finally, the Raman spectra were recorded by detuning the actuation frequency from the resonance peak. Fig. 4(c) plots the sum of the area of the three main peaks of pentacene normalized to one versus the actuation frequency, together with the pillar resonant frequency measured before the deposition of pentacene by optical lever deflection

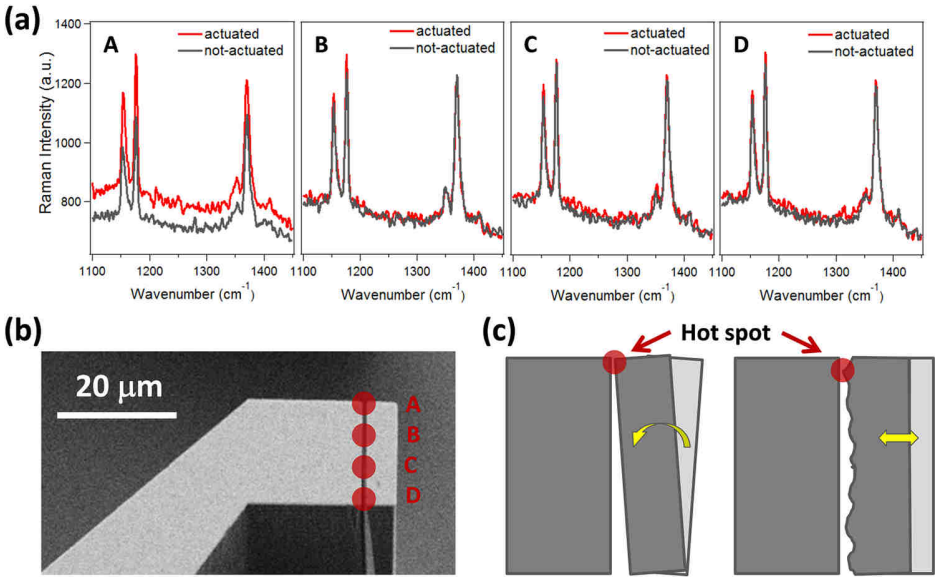

FIG. 3. (a) Raman spectra of pentacene acquired at 4 different positions along the gap (indicated as A, B, C, and D in Fig. 3(b)) in the static condition (grey line) and when the pillar is actuated at its resonant frequency at the highest amplitude (red line). The raw data show a signal increase of 40%. (b) An SEM image of the device that indicates the four positions, at which the Raman spectra have been acquired. (c) Two scenarios for the localized enhancement: left, during oscillation the pillar experiences a torsion along its z axis, due to the asymmetrical structure at its base (see Fig. 1(b)), which results in a single point of contact; right, surface roughness higher than 2 nm isolate a single point of contact.

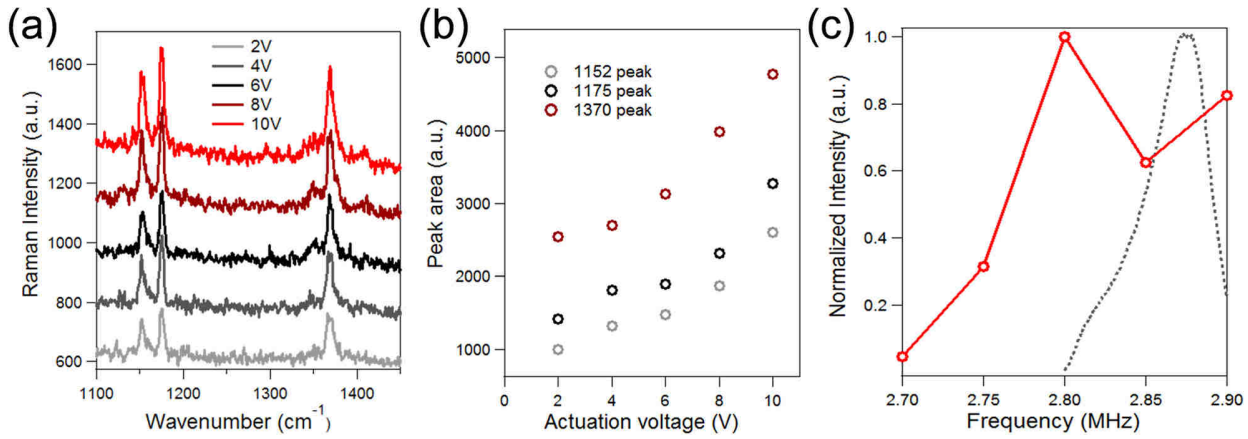

FIG. 4. (a) Raman intensities for increasing actuation amplitude. (b) Areas of the three main Raman peaks for increasing actuation amplitude: the increase in the Raman signal reflects the increase of the fraction of the oscillation period, in which the pillar is in contact with the steady wall. (c) The Raman intensity at different frequency around the resonance frequency (red continuous line) and the pillar resonant response measured with the optical lever method (black dotted line) in air.

method with actuation voltage much lower than the impact threshold.

The fact that an enhancement is obtained at one edge of the structure can be explained if we consider that (i) the pillar and the wall edges present a lateral roughness larger than a few nm, in a way that true contact is reached only at one position along the gap; (ii) the structure is not perfectly symmetrical, as clearly visible in Fig. 1(b), at the pillar base, and at the frequency, the pillar motion is a combination of a swing and a torsion motion along its main axis. These two considerations are sketched in Fig. 3(b); however, an SEM image resolution is not detailed enough to discriminate between these two cases. Strikingly, far from the edge, the Raman intensity is not affected by the oscillation that confirms that the enhancement we observed is due to the creation of hot spots in the gap and not to the bare motion or bending of the pillar at resonance.

The dependence of the enhancement at the resonance with the actuation voltage reflects the fact that for stronger actuation the contact time increases. Since impact oscillators are characterized by a chaotic motion,[19] the actual dependence of the contact time on actuation strength is still not understood; indeed, the Raman intensity measurement could provide an alternative way to investigate these phenomena.

Finally, the dependence on the actuation frequency is a further proof of the demonstration of possibility to modulate the Raman signal with a nano-mechanical device. The shift to a lower frequency with respect to the measurement with the optical lever is partially due to the mass increase produced by the pentacene deposition and partially attributed to a laser induced heating of the pillar during the Raman measurements, which require much longer integration times and laser power than optical lever method. Indeed, we observed that longer laser exposures induce pentacene desorption as a consequences of local heating.

The observed maximum increase of a factor 1.87 of the total signal under actuation condition (1370 cm^{-1} peak at 10 V of actuation) can be used to estimate the effective enhancement in the hot spots, following the same approach reported in Ref. 3. Indeed, since the whole area illuminated by the laser spot contributes to the not-actuated Raman signal and the hot spot area is limited to a 1 nm-thin line along the gap, locally the effect is much larger. We first evaluate the Raman signal coming from the hot spot region when the pillar is not-actuated as

$$\frac{S_{NA}}{A}a,$$

where A is the area of the laser spot and a is the area of the hot spot that are in our case 1 25 000 nm^2 and 400 nm^2, respectively. Then, we evaluate the increase of the Raman signal coming from the hot spot region when the pillar is actuated as

$$S_A - S_{NA} = 0.87 S_{NA},$$

where we reasonably assumed that all the Raman enhancement is originated in the hot spot region. The ratio of the latter with the previous number provides an average relative enhancement of 270. We then take into account that the hot spots are formed only during the fraction of the oscillation period, in which the pillar is closer than 1 nm to the steady wall, which is in our case approximately 5% of the period. This finally provides an actual hot spot enhancement of 5400. This represents a lower limit since we assumed that hot spots are formed along the whole length of the gap, while our observations indicate that they are concentrated in restricted regions, but the exact profile of the gap cannot be obtained with the required sub-nm precision. Further investigations with nanometer sized gold patches located near the contact point are required to obtain a more careful evaluation of the SERRS enhancement in the gap.

In conclusion, we demonstrated the integration of Raman substrates with a micromechanical device, which, when operated at its resonance frequency, can be used to modulate the Raman signal, by switching on/off the formation of the localized plasmonic hot spots. Although in our experiments the overall increase of the Raman signal amounts only to a factor of 2, a careful device design in which gold is deposited only at the pillar and hard wall facing edges would show several orders of magnitude of enhancement. Our results pave the way to the parallelization of Raman spectroscopy. Indeed, the impact resonator pillars could be fabricated in dense arrays, each with a slightly

different resonant frequency.[26] By sequentially actuating at each resonant frequency, the hot spots on an individual Raman pixel could be activated and the Raman contribution from each hot spot could be distinguished. Moreover, micromechanical frequency modulation scheme opens the way to lock-in based signal amplification in Raman detection.

See supplementary material for Duffing effect on pillar, optical absorption of pentacene film on glass, the pentacene Raman spectra with polarization parallel to the gap and on the pillar top surface far from the gap.

The financial support through the CNR-TUBITAK bilateral projects FREMORS and FORMERS (TUBITAK 113F375 and 115F603), METU Grant (BAP-01-05-2016-001) and the Italian Ministry of Education MIUR (FIRB RBAP11ETKA_003) is acknowledged.

[1]M. I. Stockman, L. N. Pandey, and T. F. George, Phys. Rev. B **53**, 2183 (1996).
[2]S. Nie and S. R. Emory, Science **275**, 1102 (1997).
[3]A. Bek, F. De Angelis, G. Das, E. Di Fabrizio, and M. Lazzarino, Micron **42**, 313 (2011).
[4]D. Naumenko, V. Zannier, V. Grillo, D. Cassese, G. Priante, S. Dal Zilio, S. Rubini, and M. Lazzarino, Nanoscale **6**, 13651 (2014).
[5]W. Zhu and K. B. Crozier, Nat. Commun. **5**, 5228 (2014).
[6]C. Sönnichsen, B. M. Reinhard, J. Liphardt, and A. P. Alivisatos, Nat. Biotechnol. **23**, 741 (2005).
[7]Q. H. Guo, C. J. Zhang, C. Wei, M. M. Xu, Y. X. Yuan, R. A. Gu, and J. L. Yao, Spectrochim. Acta A **152**, 336 (2016).
[8]H. Gehan, L. Fillaud, M. M. Chehimi, J. Aubard, A. Hohenau, N. Felidj, and C. Mangeney, ACS Nano **4**, 6491 (2010).
[9]Y. Wu, F. Zhou, L. Yang, and J. Liu, Chem. Commun. **49**, 5025 (2013).
[10]P. Taladriz-Blanco, N. J. Buurma, L. Rodrıguez-Lorenzo, J. Perez-Juste, L. M. Liz-Marzana, and P. Herves, J. Mater. Chem. **21**, 16880 (2011).
[11]L. Piantanida, D. Naumenko, E. Torelli, M. Marini, D. M. Bauer, L. Fruk, G. Firrao, and M. Lazzarino, Chem. Commun. **51**, 4789 (2015).
[12]T. R. Albrecht and C. F. Quate, J. Appl. Phys. **62**, 2599 (1987).
[13]J. Fritz, M. K. Baller, H. P. Lang, H. Rothuizen, P. Vettiger, E. Meyer, H. J. Guentherodt, Ch. Gerber, and J. K. Gimzewski, Science **288**, 316 (2000).
[14]B. Ilic, Y. Yang, K. Aubin, R. Reichenbach, S. Krylov, and H. G. Craighead, Nano Lett. **5**, 925 (2005).
[15]H. Pakdast and M. Lazzarino, Sens. Actuator, A **175**, 127 (2012).
[16]A. Qazi, D. Nonis, A. Pozzato, M. Tormen, M. Lazzarino, S. Carrato, and G. Scoles, Appl. Phys. Lett. **90**, 173118 (2007).
[17]A. B. Nordmark, J. Sound. Vib. **145**, 279 (1991).
[18]J. Ing, E. Pavlovskaia, M. Wiercigroch, and S. Banerjee, Philos. Trans. R. Soc. A **366**, 679 (2008).
[19]X. Wei, F. Bizzarri, C. Anthony, M. C. L. Ward, and D. Lowe, Micro Nano Lett. **7**, 279 (2012).
[20]M. Melli, A. Pozzato, and M. Lazzarino, Microelectron. Eng. **87**, 730–733 (2010).
[21]M. Melli, G. Scoles, and M. Lazzarino, ACS Nano **5**, 7928 (2011).
[22]S. Zaitsev, O. Shtempluck, E. Buks, and O. Gottlieb, Nonlinear Dyn. **67**, 859 (2012).
[23]H. W. C. Postma, I. Kozinsky, A. Husain, and M. L. Roukes, Appl. Phys. Lett. **86**, 223105 (2005).
[24]H.-L. Cheng, Y.-S. Mai, W.-Y. Chou, L.-R. Chang, and X.-W. Liang, Adv. Funct. Mater. **17**, 3639 (2007).
[25]D. Faltermeier, B. Gompf, M. Dressel, A. K. Tripathi, and J. Pflaum, Phys. Rev. B **74**, 125416 (2006).
[26]M. Tardivo, V. Toffoli, G. Fracasso, D. Borin, S. Dal Zilio, A. Colusso, S. Carrato, G. Scoles, M. Meneghetti, M. Colombatti, and M. Lazzarino, Biosens. Bioelectron. **72**, 393 (2015).